Doping Properties of Polydithienylmethine: A Study on the Correlation between Polymer Chain Length, Spectroscopy, and Transport

Seamus A. Curran,*,† Donghui Zhang,†,‡ Sreeker Dundigal,†,§ and Werner Blau⊥

Physics Department, New Mexico State University, Las Cruces, New Mexico 88003, Department of Chemistry and Biochemistry, New Mexico State University, Las Cruces, New Mexico 88003, Department of Electrical and Computer Engineering, Department of Physics, New Mexico State University, Las Cruces, New Mexico 88003, and Physics Department, Trinity College Dublin, Dublin, Ireland

Received: May 23, 2005; In Final Form: August 17, 2005

(1*S*)-(+)-10-Camphorsulfonic acid-doped polydithienylmethine was prepared through an acid-catalyzed condensation reaction of α,α′-di-2-thienyl-(2,2′-bithiophene)-5,5′-dimethanol and was characterized by ^{1}H NMR spectroscopy and size exclusion chromatography (SEC). The electronic and vibrational properties of the resulting polymer thin films vary with the loadings of the (1*S*)-(+)-10-camphorsulfonic acid. The dark conductivity and drift mobility, which is significantly high, of the polymer thin films were enhanced with increasing doping levels and reached maximum values of 8.0×10^{-5} S·cm^{-1} and 3.5×10^{-2} cm^2·V^{-1}·s^{-1}, respectively, at a 7 mol % dopant loading. Higher doping levels (>7 mol %) result in nonuniform polymer thin films with degraded optical quality due to the formation of nanocrystalite and thus a decrease in conductivity and drift mobility was observed. The doped polydithienylmethine thin film also exhibited a photoconductivity response with an excitation at 457 nm and the highest photoconductivity (2×10^{-4} S·cm^{-1}) was again observed at the 7 mol % doping level. Spectroscopic investigation suggests that the enhanced transport properties can be attributed to polaronic species present. The electronic and vibrational changes which relate to such doping were characterized by electronic absorption spectroscopy, Raman spectroscopy, and FTIR spectroscopy. The changes in transport values can be directly related to the changes we see in our spectroscopic investigations.

1. Introduction

Since the initial discovery of conducting polymers, specifically polyacetylene, intensive work has been carried out to find uses applicable to their unique properties including physical flexibility, tailorability of their optical and electronic properties, low synthesis costs, etc.[1−5] However, one of the problems associated with many conducting polymers is their poor solubility in common organic solvents, thus hindering their processibility. The common approaches for enhancing polymer solubility are either through incorporation of solublizing substituents onto the polymer backbone or addition of surfactants. Heeger and co-workers have demonstrated that by using an appropriate acid to protonate polyaniline (PANI), the counterion can enable the solubility of the resulting PANI complex in a variety of organic solvents and induce processibility.[6−8] Furthermore, addition of protonic source (dopant) is known to enhance the polymer conductivity, which is much desirable in many electronic applications.

In the area of polymer electronics such as light emitting diodes (LEDs) and solar cell production, polythiophenes, polyisothionaphthlenes, and in particular PANI have been extensively studied and demonstrated great potentials for commercial purposes.[9−16] Theoretical calculation predict that conjugating polymers with structures as shown in Figure 1a could have a small band gap at about 1 eV and that they would be very good conductors with conductivity potentially as high as 10^{-3} S·cm^{-1} due to their quinoid and aromatic structures.[17−19] It also has been observed that the band gap of polymers decreases with increasing quinoid structures present along the polymer π conjugated backbone.[20] Thus, we are interested in studying the properties of polydithienylmethine, which is essentially a structural analogue of polythiophene with additional quinoid structures.

2. Experimental Section

α,α′-Di-2-thienyl-(2,2′-bithiophene)-5,5′-dimethanol, (1*S*)-(+)-10-camphorsulfonic acid (CSA), and CH_2Cl_2 were used as received without any further purification. Depending on the required doping levels, different amounts (by molar percentage, mol %) of camphorsulfonic acid were added to a CH_2Cl_2 (20 mL) solution of α,α′-di-2-thienyl-(2,2′-bithiophene)-5,5′-dimethanol (0.5 g, 1.3 mol). The reaction mixture was stirred at room temperature for 24 h and the solution turned dark brownish black. Then the solvent was removed under vacuum to afford the doped polymer as a black glassy solid. It was previously reported that treatment of α,α′-di-2-thienyl-(2,2′-bithiophene)-5,5′-dimethanol films with trifluoroacetic acid vapor as a catalyst yields polydithienylmethine polymer films (Figure 1b) that are of good standard in terms of uniformity and optical quality.[21,22] However, physical characterizations of resulting polymer films, such as determination of molecular weight and measurement of nonlinear optical properties, were impeded due to its insolubility. It was also demonstrated that addition of surfactant to insoluble conducting polymers can sometimes improve their

* To whom correspondence should be addressed. E-mail: shay@physics.nmsu.edu.

† Physics Department, New Mexico State University.

‡ Department of Chemistry and Biochemistry, New Mexico State University.

§ Department of Electrical and Computer Engineering, Department of Physics, New Mexico State University.

⊥ Physics Department, Trinity College Dublin.

10.1021/jp052711v CCC: $33.50
Published on Web 02/03/2006

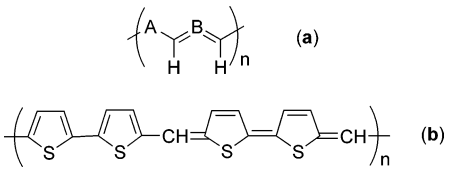

Figure 1. Graphic representation of (a) polyarenemethine where A and B are aromatic rings such as benzene or pyrrole and (b) polydithienylmethine.

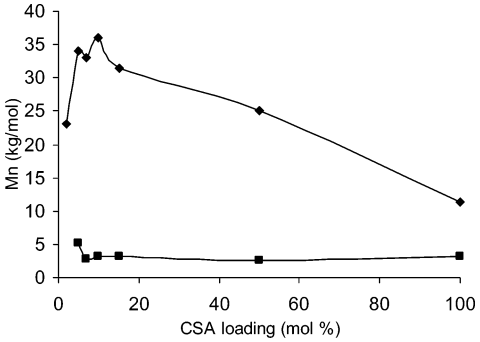

Figure 2. Molecular weights of CSA-doped polydithienylmethines at different CSA loadings: (◆) high M_n fraction and (■) low M_n fraction.

solubility.[6] Thus, we decided to investigate camphorsulfonic acid (CSA) as a surfactant for solublizing polydithienylmethine. Additionally, CSA possesses a sulfonic acid functional group, which can readily catalyze the formation of polydithienylmethine from α,α′-di-2-thienyl-(2,2′-bithiophene)-5,5′-dimethanol.

Indeed, addition of CSA to a CH_2C1_2 solution of the α,α′-di-2-thienyl-(2,2′-bithiophene)-5,5′-dimethanol resulted in the immediate formation of a homogeneous solution with a blue coloration. The color of the solution gradually darkened, but the solution remained homogeneous throughout the reaction course without noticeable precipitation, which indicates that the product polymer was solublized by the CSA. After 24 h, the product polymer was isolated by removing the excess solvent. ^{1}H NMR spectrum of the final product indicated the complete formation of the desired polymer doped with CSA. Polydithienylmethine samples with different CSA loadings were prepared in the same fashion and the molecular weights of the polymers were determined by size exclusion chromatography (SEC) in reference to polystyrene standards. The molecular weight (M_n) of the resulting polymer samples varies with CSA loadings (Figure 2) and exhibits an interesting bimodal distribution except for the one with 2 mol % CSA loading. So far, we have not been able to separate the high and low molecular weight portions although a number of synthetic and chromatographic techniques have been attempted. The origin of the bimodal distribution of molecular weights is not clear, yet its importance cannot be neglected because polymer molecular weight can significantly influence its electrical, optical, and mechanical properties.

3. Results and Discussion

3.1. Electronic Absorption Spectroscopy (Vis−Near-IR Region). The absorption spectra in the visible/near-infrared region (400−1600 nm) were collected for polydithienylmethines doped with various amounts of CSA (2 to 100 mol %). In all spectra, there are three observable absorption bands with two centered at 1200 (1.03 eV) and 1400 nm (0.89 eV) in the near-infrared region and the third shifting in the region between 525 (2.36 eV) and 438 nm (2.83 eV) dependent on the CSA loading. Another feature to note in the spectra is the appearance of a shoulder in the absorption around 500 nm as the CSA loading

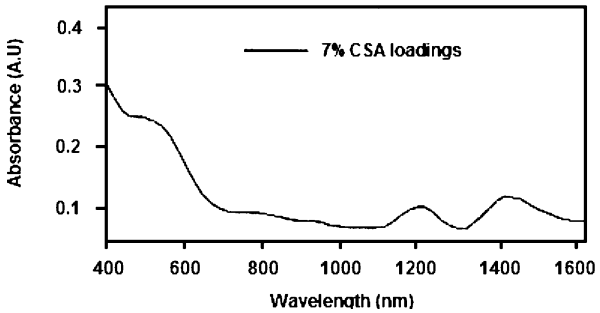

Figure 3. The electronic absorption spectrum of 7 mol % CSA doped polydithienylmethine in the visible−near-IR region.

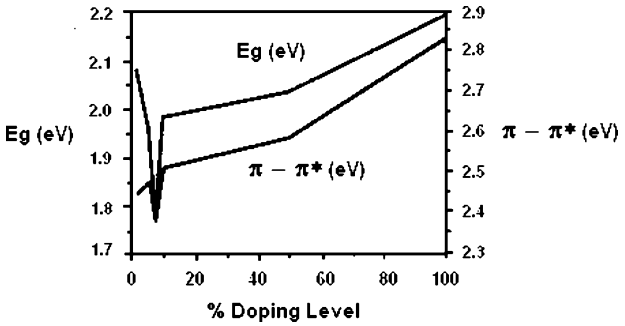

Figure 4. Dependence of band gap (E_g) and $\pi-\pi^*$ absorptions on CSA doping level.

increases (Figure 3). This feature is most evident for the sample with 7 mol % CSA loading. As the CSA loading increases further, this feature gradually disappears. The most probable explanation of this is a $\pi-\sigma^*$ or $\sigma-\pi^*$ transition, which is more evident in the samples where the molecular weight is higher, this feature being not so evident in solutions of lower molecular weight.

The band gap can be assigned to the higher wavelength edge of the third main absorption due to $\pi-\pi^*$ transition before it tails off. The band gap exhibits a dependency on the CSA loading (Figure 4) with the lowest band gap (1.76 eV) at 7 mol % CSA loading and the highest (2.19 eV) at 100 mol % CSA loading. Although previous calculations by Brédas et al predicted a 1 eV band gap for this type of polymer,[17] π-conjugations with different chain length can alter the band gap significantly. The SEC results have shown that CSA-doped polydithienylmethine samples consisted of a high molecular weight portion and a low molecular weight portion. Thus, the reduced band gap can arise due to the presence of high molecular weight polydithienylmethines. Both the band gap and the $\pi-\pi^*$ position show similar responses energetically, similar to the response of the GPC results.

3.2. Raman Spectroscopy. Raman spectra of polydithienylmethines doped with different CSA loading were collected at an excitation wavelength of 514.5 nm. The dominating Raman features are in the region between 1400 and 1600 cm^{-1}, and are attributed to various resonantly enhanced C═C stretching modes tentatively designated as the quinoid ring-stretching mode (ν_{quin}), the thiophene ring-stretching mode (ν_{ring}), and the inter-ring-stretching mode (ν_{inter}). Several Raman lines with weaker intensity appear at lower wavenumbers (400−1200 cm^{-1}), originating from different C═C deformations, C═C bending, and other modes. Similar features were also observed in other conjugated polymers such as polythiophene or polyisothianaphthene.

A Lorenzian curve fit in the spectral region for the C═C stretching mode afforded Raman lines at 1422, 1455, 1495,

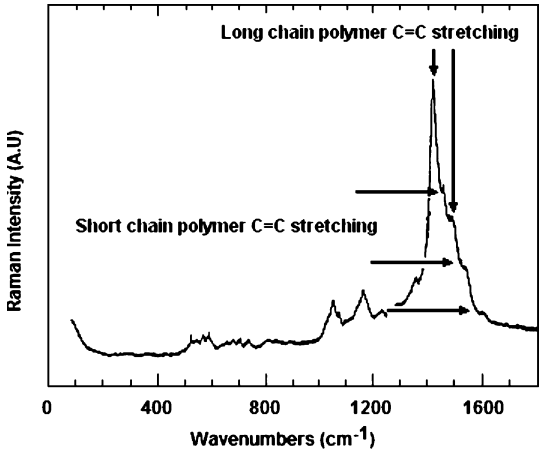

Figure 5. Raman spectrum of CSA doped polydithienylmethines, with the bimodal distribution affecting the position of the C═C stretching modes, using the 514.5 nm excitation line.

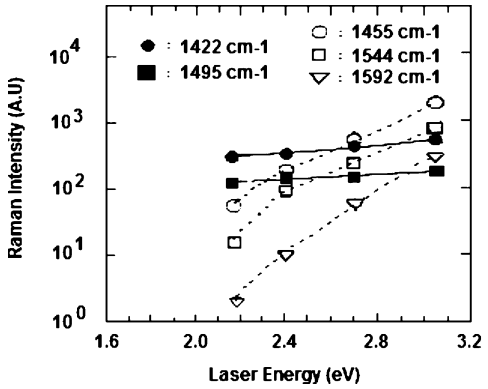

Figure 6. Dependence of Raman intensities on excitation energy of laser beams.

1544, and 1592 $cm^{-1,}$ respectively (Figure 5). One feature to note is that the Raman lines between 1400 and 1600 cm^{-1} are not dispersive, as no apparent shift of line positions was observed when we vary the excitation energy of the laser beams. This suggests that these Raman lines arise from the first-order resonance scattering process and are due to the symmetry-allowed C═C stretching modes of thiophene ring and quinoid structures. But the relative intensities of these lines changed dramatically. Two groups of lines can be clearly distinguished by their intensity dependence on excitation energy (Figure 6). The first group at 1422 and 1495 cm^{-1} are the most intense after excitation with the yellow (568.2 nm) or green (514.5 nm) laser, whereas a second group at 1455, 1544, and 1592 cm^{-1} dominates upon excitation with the blue lasers (457.9 and 406.8 nm).

The different resonance Raman behavior for the two groups of lines can be explained by taking into account the bimodal distribution of the polymer conjugation length. The polymers consist of two fractions, one with a much longer conjugation length than the other. The Raman lines at 1422 and 1495 cm^{-1} originate from the former, since in such a case electronic transition energies are red shifted as compared to short polymer chains and thus even after excitation with the yellow laser these lines have considerable intensities. As a corollary, the lines at 1455, 1544, and 1592 cm^{-1} can be assigned to the short polymer segments. Although this gives six different lines of which five are observed the sixth line is probably dominated by one of the strong lines.

3.3. FT-IR Spectroscopy. CSA-doped polydithienylmethine prepared with NaCl plates was examined for FTIR activity

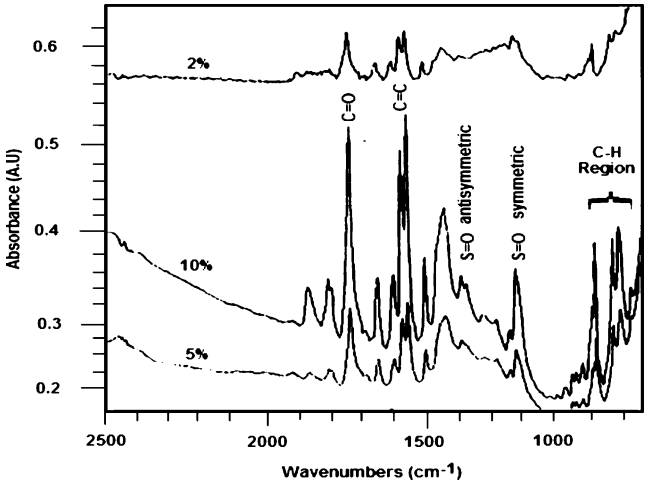

Figure 7. FT-IR spectra of polydithienylmethines with loadings from 2 to 10 mol % of CSA. The spectrum also shows the position of different vibrational modes associated with the changes induced by doping.

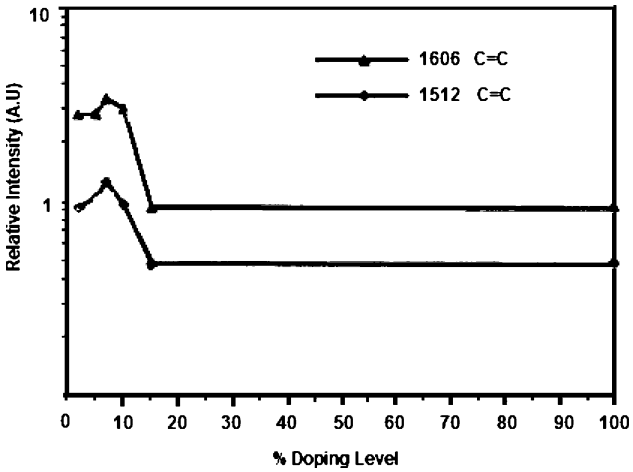

Figure 8. Comparison of FT-IR intensity changes of the $\nu_{C=C}$ stretching mode with increased CSA loadings.

between 5000 and 500 cm^{-1} (Figure 7). The presence of dopant CSA was confirmed by the peaks at 1169 and 1350 cm^{-1} due to the symmetric and anti-symmetric S═O stretching modes of the sulfonic acid group, and peaks at 1746 and 1773 cm^{-1} due to the C═O stretching modes. In addition, C−H bending and deformation modes were assigned in the fingerprint region (700−1000 cm^{-1}) as well as the C−H stretching modes at about 3000 cm^{-1}. One interesting feature to note is that the intensity of C═C stretching modes can be correlated with the changes of polymer conjugation length. For instance, the peak located at 1512 and 1606 cm^{-1} associated with C═C stretching modes initially grows slightly from the 2 to 10 mol % CSA doping level.

Show in Figure 8 are the different C═C vibrational lines with increasing CSA loadings. The trend we see in the changes in relative intensity of these lines is similar to that observed for molecular weight of the polymer with different CSA loadings, and this is a reliance on the chain length we have measured in GPC. It can be understood that as the doping increases, the relative conjugation length indicated by the 1606 cm^{-1} C═C line increases until the 10% doping level is reached. At this point the peak decreases rapidly in intensity due to shortening of the conjugation, which was observed from GPC measurements. This is a typical response for conjugated polymers in

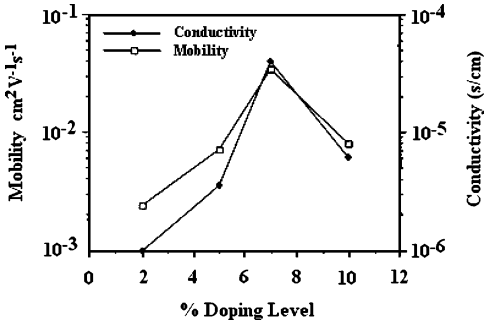

Figure 9. Dependence of conductivity and drift mobility on the CSA doping level.

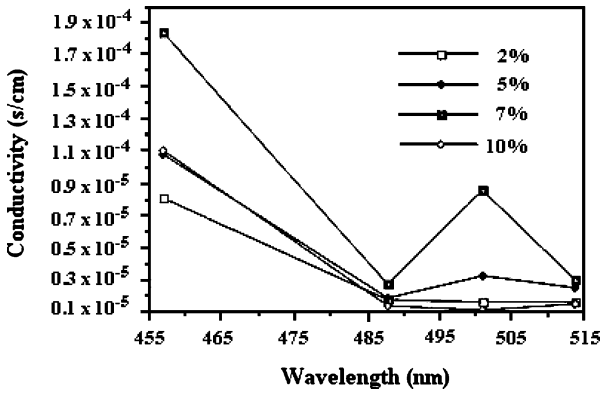

Figure 10. Dependence of photoconductivity on excitation energy of different laser beams.

that when polymers increase in length a corresponding increase in the C═C peak height occurs.

3.4. Transport Properties. *3.4.1. Dark Phase Response.* Dark conductivities of CSA-doped polydithienylmethine thin film (prepared by drop casting over the contacts) were measured by using a two-probe method at different CSA loadings. The polymer conductivity exhibits a nonlinear dependency on CSA loading (Figure 9). At lower CSA loading levels (<7 mol %), the conductivity increases with increased CSA loading from 1×10^{-6} S·cm^{-1} for 2 mol % CSA loading to 4×10^{-5} S·cm^{-1} for 7 mol % CSA loading, which evidently indicates the dopant role of CSA. At the 10 mol % doping level, the conductivity decreases to 6×10^{-6} S·cm^{-1}. From further analysis of doping at higher concentrations of CSA, the conductivity decreased by 3 orders of magnitude at the 100 mol % CSA doping level. By using a two-point probe conductivity method, changes in CSA loadings may also be reflected in the change of contact resistance. Using the two-point probe method then easily allows for the photoresponse to be measured, and while there is greater contact resistance changes in this method as compared to four-point probe techniques, this resistance is negligible when compared to the resistance of the polymer.

Similar dependency on CSA loading was also observed for the drift mobility μ, which is equal to the free carrier mobility μ_o multiplied by the fraction of free carriers θ (Figure 3). The highest drift mobility was calculated to be 3.45×10^{-2} cm^2·V^{-1}·s^{-1} at 7 mol % CSA loading, using eq 1:

$$J = A\mu\epsilon\epsilon_0 V^2/L^3 \quad (1)$$

where J is the current density, A is a constant, μ is the drift mobility, ϵ and ϵ_0 are the dielectric constant of polymer and free space, respectively, V is the applied voltage, and L is the distance between the electrodes.

The dependence of conductivity as well as the drift mobility on CSA loadings is accounted for by the presence of different polymer conjugation length. Similarly, the conductivity can also be related to the presence of both short chains and long chains present. Although there are no short chains present with the 2 mol % doping level the polymer is substantially shorter than the other doping levels and thus a lower conductivity would be expected. However, at the 5 mol % doping level, the distribution between short chains and long chains is increased substantially and thus the conductivity increase as compared to that at the 2 mol % doping level is not as dramatic as would be expected when only the difference of long chain length for 2 and 5 mol % doping levels was taken into account. At the 7 mol % doping the ratio between short chains and long chains is at its smallest and thus a greater conductivity is observed than that of the 5 mol % doping. For the 10 mol % doping level, although the long chain weight is increased so too is the short chain increased, which will inhibit the carrier transfer. At a CSA level higher than 10 mol %, film formation begins to deteriorate. The polymer film becomes nonuniform and microcrystallite formation was observed. Those microcrystallites, which are crystallized amalgams of polymer and CSA, can act as physical trapping sites for current carrying carrier and a reduced conductivity will result. The presence of defects is also suggested by the presence of the second conduction regime due to space charge limited current, which also enables us to calculate the drift mobility using eq 1.

3.4.2. Photoconductive Response. Polydithienylmethines with 7 mol % CSA loading were excited at a number of wavelengths to obtain the optimum wavelength for the most increased photocurrent. A typical I/V characteristic was obtained from a sandwich cell configuration, where the polymer lay between the gap of the two electrodes. Within this gap the polymer was illuminated from the backside of the substrate and sufficient care was taken to prevent the electrodes from being illuminated. The polymer was photoexcited, which resulted in the generation of charged carriers and increased the overall carrier production so that a greater current is obtained compared to the dark current generation. The current enhancement can be viewed simply as energy taken in by the polymer in the ground state which promotes the generation of carriers similar to that of an applied electric field.[23−27]

The polymer was irradiated at a number of different wavelengths, and all photoexcitation energies were greater than that of the band gap transition energy of 1.76 eV. The results of these experiments can be seen in Figure 10 where the conductivity is plotted against different wavelengths for four different doping levels. By examining the shape of the photoconductivity curves it can be seen that they resemble very closely the absorption spectrum shape within this energy region. Using the AlGaAs laser with a wavelength output of 815 nm photoconductivity was observed, although very small, and only slightly greater (about 1.5% increase) than the dark conductivity result. This means that the onset of photoconduction occurs at the fundamental absorption edge. Comparison of the spectral response of photoconductivity with the absorption spectrum near the absorption edge provides vital evidence of the nature of the charged carriers. Similar to the response found in polydiacetylene,[28] the interband transition can be explained in terms of either free carriers or alternatively exciton generation, which breaks into two components: electrons and holes.[29] The conventional concept for photoconductivity via an interband transition predicts a threshold energy for free carrier generation at the fundamental optical absorption edge with relatively high sensitivity for $h\nu$ at photon energies above E_g. The carrier photogeneration rate is proportional to the number of photons absorbed. A peak would

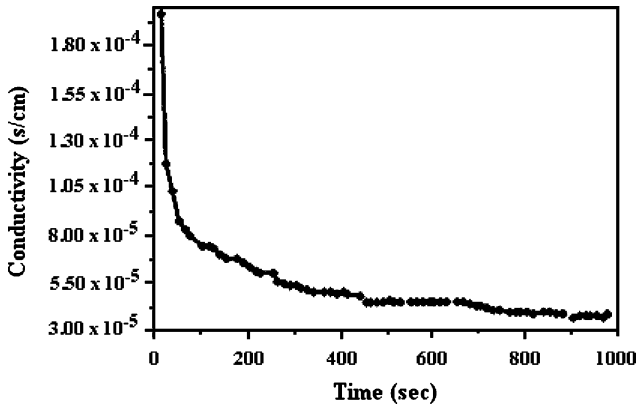

Figure 11. Time dependence of conductivity relaxation for the 7 mol % CSA doped polydithienylmethine.

be expected for thin films at the wavelength corresponding to the maximum in the absorption spectrum. This can be clearly observed for polydithienylmethine in that, for all doping levels, the maximum photoconductivity with excitation at 457 nm mirrors that of the maximum absorption observed in the blue region. The photoconductivity obtained is at least 1 order of magnitude greater that the dark phase conductivity. If irradiation was attempted through a thick film where the thickness was much larger than the optical absorption depth the photocurrent would then be insensitive to the photon frequency for energies greater than the energy gap. To ensure exact determination of the carrier present illumination should be maintained either at the film surface and examined as a surface effect or from a region with transmission to the polymer between the electrodes. On the other hand, if the absorption was excitonic in nature then there would be no photoconductivity until the photon energy was sufficient to overcome the exciton binding energy and generate free carriers.[30] Typically, this would correspond to the onset of photocurrent at a higher energy than the fundamental absorption edge, which is not the case for our CSA doped polydithienylmethine samples.

3.4.3. Time Response. Over a period of time the dark conductivity of the 7 mol % doped sample was found to decrease by an order of magnitude from 1.95×10^{-5} S·cm^{-1} to about 2×10^{-6} S·cm^{-1} (Figure 11). This was also found to hold true for all sample treated with CSA and this decrease occurred in just over 15 min where the readings were taken roughly every 20 s. The initial decrease in conductivity was very fast—over half the initial value was lost in a matter of 20 s. Then the conductivity stabilized so the rate of decay decreased substantially after 300 s. This behavior suggests that steady state conductivity always decreases, which can pose a problem for device applications where steady state currents are required to vary only slightly over a long duration.

After termination of illumination the photoinduced conductivity exhibits relaxation and in the long time regime follows the stretched exponential form (eq 2) similar to that seen in the dark phase.

$$\sigma(t) = \sigma_0 \exp[-(t/\tau)^{\beta}] \qquad 0 < \beta < 1 \tag{2}$$

Nonexponential relaxation toward equilibrium has been observed in a wide range of systems.[31,32] The slow decay of photocurrent is indicative of persistent photoconductivity observed in some organic semiconductors.[30] After a fast initial decay the excess photoconductivity approaches equilibrium as in the case of the dark current decay. This type of decay has been observed for all doping levels. The instantaneous lifetime is defined as:

$$\tau_{ins} = \sigma/[d\sigma(t)/dt] \tag{3}$$

By examining the instantaneous lifetime, we are able to gain some insight into the nature of the conductivity relaxation process. For a monomolecular process, the instantaneous lifetime is a constant for the exponential decay with a single lifetime and is linearly proportional to t in the case of bimolecular recombination. In our case, the instantaneous lifetime is a sublinear function of time, $\tau_{ins} \sim t^{\alpha}$ with $0 < \alpha < 1$, which indicates that recombination of the photoexcited carriers is restricted due to doping sites present within the band gap, which prevent relaxation of carriers to the ground state.

In all the conductivity measurements, low electronic field was used and we did not observe any noticeable degradation of the polymer films. Thus, we argue that electrochemical degradation of the polymer films is very unlikely. One possible cause for the decay process is that the polarons may recombine to form bipolarons.[33−35] Such recombination has been reported to be a diffusion rate-limited process and has a power law dependence (τ^{-n}) of between $\tau^{-0.4}$ and $\tau^{-0.6}$. By plotting $[-di/dt]$ against t for all samples measured, n values ranging between 0.33 and 0.56 were obtained. This behavior is indicative of the trapping behavior and its effect on the mobility in the bulk polymer.

4. Conclusion

Insoluble systems such as the polymer polydithienylmethine can be solubilized by using a sulfonic acid based system such as CSA. Characterization of the solublized polydithienylmethine samples by size exclusion chromatography suggested that the polymers consist of two fractions, one with high molecular weight and the other with low molecular weight (a factor of ~10 lower). In addition, the presence of the CSA enhanced the conductivity and drift mobility of the polymer by introducing polaronic species to the polymer matrix. The bimodal distribution of polymer conjugation lengths affected the transport properties and was observed spectroscopically. Changes in the band gap and the presence of polaronic species can be spectroscopically correlated to the changes in transport mechanisms. We see that while the conductivity of the polymer is low and directly related to the changes in chain lengths and doping levels, the mobility of the polymer is very high suggesting that chain length and carrier mobility are not directly related. Further study of this phenomenon is underway.

References and Notes

(1) Willersinn, H.; Naarmann, H.; Schneider, K. DE 1953898, 1971.
(2) Lee, D.; Swager, T. M. *J. Am. Chem. Soc.* **2003**, *125*, 6870.
(3) Dimitriev, O. P. *Macromolecules* **2004**, *37*, 3388.
(4) DuBois, C. J.; Abboud, K. A.; Reynolds, J. R. *J. Phys. Chem. B* **2004**, *108*, 8550.
(5) Han, C.-C.; Lu, C.-H.; Hong, S.-P.; Yang, K.-F. *Macromolecules* **2003**, *36*, 7908.
(6) Cao, Y.; Smith, P.; Heeger, A. J. *Synth. Met.* **1992**, *48*, 91.
(7) Polk, B. J.; Potje-Kamloth, K.; Josowicz, M.; Janata, M. *J. Phys. Chem. B* **2002**, *106*, 11457.
(8) Potje-Kamloth, K.; Polk, B. J.; Josowicz, M.; Janata, M. *Chem. Mater.* **2002**, *14*, 2782.
(9) Burroughs, J. H.; Bradley, D. D. C.; Brown, A. R.; Marks, R. N.; McKay, K.; Friend, R. H.; Burn, L. P.; Holmes, A. B. *Nature* **1990**, *347*, 539.
(10) Braun, D.; Heeger, A. J. *Appl. Phys. Lett.* **1992**, *58*, 1982.
(11) Tan, S.; Zhai, J.; Xue, B.; Wan, M.; Meng, Q.; Li, Y.; Jiang, L.; Zhu, D. *Langmuir* **2004**, *20*, 2934.
(12) Carswell, A. D. W.; O'Rear, E. A.; Grady, B. P. *J. Am. Chem. Soc.* **2003**, *125*, 14793.
(13) Schwendeman, I.; Hickman, R.; Sonmez, G.; Schottland, P.; Zong, K.; Welsh, D. M.; Reynolds, J. R. *Chem. Mater.* **2002**, *14*, 3118.

(14) Kido, J.; Kimura, M.; Nagai, K. *Science* **1995**, *267*, 1332.
(15) Brotherston, I. D.; Mudigonda, D. S. K.; Osbron, J. M.; Belk, J.; Chen, J.; Loveday, D. C.; Boehme, J. L.; Ferraris, J. P.; Meeker, D. L. *Electrochim. Acta* **1999**, *44*, 2993.
(16) Arbizzani, C.; Mastragostino, M.; Zanelli, A. *Sol. Energy Mater. Sol. Cells* **1995**, *39*, 213.
(17) Toussaint, J. M.; Themans, B.; André, J. M.; Brédas, J. L. *Synth. Met.* **1989**, *28*, 205.
(18) Bourdin, E.; Curran, S.; Blau, W.; Blöchl, G.; Becker, R. *Synth. Met.* **1993**, *57*, 5052.
(19) Bourdin, E.; Curran, S.; Davey, A. P.; Blau, W.; Blöchl, G.; Becker, R.; Bräunling, H. *Adv. Mater. Opt. Electron.* **1993**, *4*, 43.
(20) Adant, C.; Brédas, J. L. Private communication, Rochester, 1994.
(21) Bräunling, H.; Blöchl, G.; Becker, R. *Synth. Met.* **1991**, *41*, 487.
(22) Bräunling, H.; Becker, R.; Blöchl, G. *Synth. Met.* **1993**, *55*, 833.
(23) Chance, R. R.; Baughman, R. H. *J. Chem. Phys.* **1976**, *64*, 3889.
(24) Egbe, D. A. M.; Cornelia, B.; Nowotny, J.; Gunther, W.; Klemm, E. *Macromolecules* **2003**, *36*, 5459.
(25) Egbe, D. A. M.; Bader, C.; Klemm, E.; Ding, L.; Karasz, F. E.; Grummt, U.-W.; Birckner, E. *Macromolecules* **2003**, *36*, 9303.
(26) Lee, G. J.; Kim, K.; Jin, J.-I. *Opt. Commun.* **2002**, *203*, 151.
(27) Abdou, M. S. A.; Orfino, F. P.; Son, Y.; Holdcroft, S. *J. Am. Chem. Soc.* **1997**, *119*, 4518.
(28) Donovan, K. J.; Wilson, E. G. *J. Phys. C*: *Solid State Phys.* **1979**, *12*, 4857.
(29) Siddiqui, A. S.; Wilson, E. G. *J. Phys. C*: *Solid State Phys.* **1979**, *12*, 4237.
(30) Lee, C. H.; Yu, G.; Heeger, A. J. *Phys. Rev. B* **1993**, *47*, 15543.
(31) Hunt, I. G.; Bloor, D.; Movoghar, B. *J. Phys. C*: *Solid State Phys.* **1983**, *16*, L623.
(32) Hunt, I. G.; Bloor, D.; Movoghar, B. *J. Phys. C*: *Solid State Phys.* **1985**, *18*, 3497.
(33) Kaufman, J. H.; Colaneri, N.; Scott, J. C.; Kanazawa, K. K.; Street, G. B. *Mol. Cryst. Liq. Cryst.* **1985**, *118*, 171.
(34) Oyaizu, K.; Iwasaki, T.; Tsukahara, Y.; Tsuchida, E. *Macromolecules* **2004**, *37*, 1257.
(35) Buga, K.; Kepczynska, K.; Kulszewicz-Bajer, I.; Zagorska, M.; Demadrille, R.; Pron, A.; Quillard, S.; Lefrant, S. *Macromolecules* **2004**, *37*, 769.